Analysis of the electron temperature measurement in TCABR tokamak by Electron Cyclotron Emission and Infrared Thomson scattering diagnostics

O C Usuriaga[1], F O Borges[1], A G Elfimov[1], R P da Silva[1], M H Ono[1], P G P P Puglia[1], M P Alonso[2], J H F Severo[1], I C Nascimento[1], E K Sanada[1], W P de Sá[1], R M O Galvão[1,3], J I Elizondo[1].

[1]Institute of Physics, University of São Paulo, SP, Brazil.
[2]Associação EURATOM/IST, Instituto de Plasmas e Fusão Nuclear - Laboratório Associado, Instituto Superior Técnico, 1049-001 Lisboa, Portugal.
[3]Brazilian Center for Physics Research, Rio de Janeiro, RJ, Brazil.

E-mail: usuriaga@if.usp.br

Abstract. This work presents the experimental analysis of the central electron temperature measured by the electron cyclotron emission (ECE) radiometer and the infrared Thomson Scattering (ITS) diagnostic. The detection of the ECE radiation is done by a heterodyne scanning radiometer that works at the second harmonic extraordinary mode, in frequency range from *50* to *85GHz*, which allows measurement of the radial profile of electron temperature with good spatial and temporal resolutions. The ITS diagnostic uses a Neodymium Glass laser (wavelength *1.054 μm*). This ITS diagnostic measures the electron temperature in the center of plasma column one time during plasma shot. Results also show a discrepancy between the two diagnostics in the electron temperature measurement in the presence of Magnetohydrodynamics activity that gives an explanation for this apparent inconsistency.

1. Introduction

The TCABR tokamak in operation at the Institute of Physics of University of São Paulo (main parameters: Major radius $R_0 = 61.5\ cm$, Minor radius $a = 18\ cm$, Plasma current $I_P < 120\ kA$, Plasma current duration $t_P < 150\ ms$ and Toroidal magnetic field $B_0 = 1.14\ T$) has a broad scientific research program that includes interaction of RF waves [1 and 2], magnetic islands and MHD oscillations [3 and 4], transport barriers by electrically polarized electrode [5] and plasma rotation [6, 7 and 8]. TCABR tokamak is equipped with a wide variety of diagnostics, being the Electron Cyclotron Emission (ECE) and infrared Thomson scattering (ITS) diagnostics used to measure of the plasma electron temperature.

The ECE radiometer has long been the only diagnostic for providing the electron temperature of plasma in tokamak TCABR. This radiometer has the major drawback of the impossibility of measuring the electron temperature beyond the cutoff density due to the conditions of accessibility. This restriction of access due to the low toroidal field, *1.14T*, imposes a limit on the measurement of electron temperature. So we can only use this diagnostics for electron densities less than $2.5\times10^{19}\ m^{-3}$ in the central position of the plasma column. This value is lower than required for most research in TCABR, such as interaction with biased electrode where the electron density in the center of the

plasma to reach a value of up to 4.0×10^{19} m^{-3}. This limitation causes, for practical purposes, this diagnostic is of limited use.

Recently, in collaboration with the Instituto Superior Técnico in Lisbon, has made it possible to install a new system for the diagnostic of electron temperature using Thomson scattering. This system allows the measurement of electron temperature in the center of the plasma column in a given time regardless of the value of the electron density. Preliminary results on the measurement of electron temperature in the central column of plasma, have been obtained using both diagnostics [9]. These initial results showed an acceptable agreement for discharges during ohmic heating and a discrepancy with Alfvén waves. Continuing to collect data for different situations TCABR plasma, we found some systematic differences in the value of electron temperature provided by both diagnostics. It was noted that this discrepancy is directly related to the presence of strong MHD activity. In this paper we present the situations in which there is agreement and disagreement between measurements made by both diagnostics and give a possible explanation for the apparent dual behavior.

2. Measurement of electron temperature from ECE emission

The detection of ECE radiation is done by means of a heterodyne scanning radiometer that works at the second harmonic extraordinary mode (*X-mode*) with frequency range from *50* to *85GHz*, which allows measurement of the radial profile of electron temperature with good spatial and temporal resolutions. The system can operate in a fixed frequency mode (time resolution *10* μs), or in a sweeping mode that allows the radial temperature profiles to be obtained. Since the radial resolution at the center of the plasma column of *1.1 cm* for toroidal field $B = 1.14T$, and circular cross section beam *~3.8* cm^2. The plasma millimeter-wave emission is received by a Gaussian Antenna located in the equatorial plane at the TCABR of the vacuum vessel.

In tokamak machines with low toroidal magnetic fields and high plasma densities, such as the TCABR tokamak, the accessibility conditions impose restrictions to the detection of the ECE. The accessibility conditions are examined based on the model of *cold plasma approximation* to describe the propagation of microwaves through the plasma. From numerical calculations it was found for the TCABR, due to the harmonic overlapping (Fig. 1a), the detection of the second harmonic, in the lower field side, is limited to the *52-74 GHz* band (*~70%* of the plasma column, which correspond to the radial range between approximately *12 cm* and *-8 cm*).

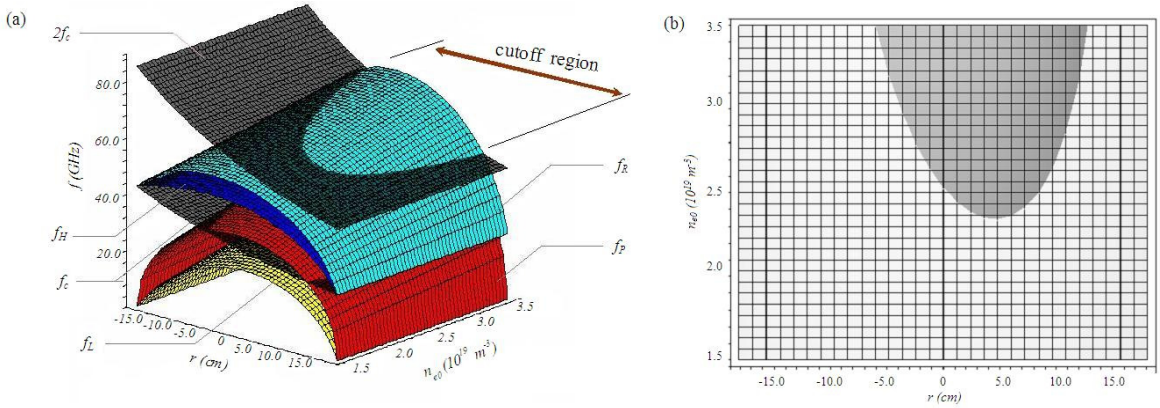

Figure 1. (a) The harmonic overlapping and cutoff frequencies for the TCABR plasma. Frequencies involved are $f_{c,}$ cyclotron frequency, $f_{P,}$ plasma frequency, $f_{H,}$ upper hybrid frequency, $f_{L,}$ left hand frequency, and $f_{R,}$ right hand frequency. (b) The area in gray color represents the region not accessible by the second harmonic plasma frequency.

The accessibility conditions for the second harmonic (X mode) restrict the maximum electron density to values bellow $n_{e0}=2.5\times10^{19}$ m^{-3}, as can be seen in Fig. 1b. Due to this cutoff, the electron temperature cannot be measured for densities greater than this.The ECE radiometer has been

calibrated absolutely; the method used basically consists in determining the output voltage of the radiometer as a function of frequency for two blackbodies with different temperatures [10]. From the results it appears that the accessibility conditions determined by the electron density and magnetic field in plasma TCABR, impose limitations on the use of the ECE diagnostic. However, the measure of electron temperature for densities below the cutoff region has been very useful in experiments in TCABR, even as the opposite of ITS where the temperature measurement is made in a single instant of time, the ECE diagnostics provides the electron temperature throughout the plasma discharge.

3. Measurement of electron temperature from Thomson scattering

The infrared Thomson scattering diagnostic is based upon a Neodymium Glass Laser with up to *4.5 Joules* per laser pulse which has a duration of approximately *50 ns*. The laser emission has central wavelength in the infrared part of the spectrum, $\lambda = 1.054\ \mu m$, and *2 nm* spectral width at half height.
In Thomson scattering experiments, the radiation from a high-energy pulsed laser is vertically directed into the Tokamak plasma. The spectrum of scattered radiation is analyzed at 90^o by simple collecting objective composed by one plan-convex and one plan-aspherical lens. The electron temperature can be determined from shape of the measured Thomson spectrum. A full description of infrared Thomson scattering diagnostic is given in ref. [9]. The infrared Thomson scattering system is shown in Fig. 2. A collection fiber transport the collected light to a set of 3-channel filtered polychromator that use avalanche photodiode detectors (APDs), ref. [11]. The scattered radiation is measured by polychromator and digitized by oscilloscope. Analyzing the signal-ratio of the detector signals (Fig. 3) we can obtain the electron temperature in center of plasma column during one plasma shot with a spatial resolution of *≈18 mm* height and *≈3 mm* diameter.

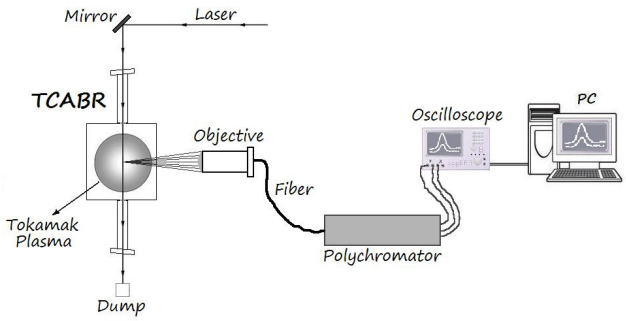

Figure 2. Schematic layout of TCABR infrared Thomson scattering system.

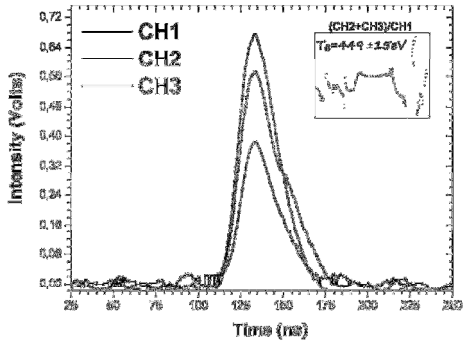

Figure 3. Thomson scattering signals from 3-channels polychromator. The lower graph is the signals-ratio.

4. Results

Figure 4 shows the results of measurements on the line-averaged electron density in the center of the plasma column and electron temperature in the same region measured by the ECE diagnostic. The lines indicate fits through the data. The top graphic shows the line-averaged density versus current plasma, and the bottom graphic shows the electron temperature versus the current plasma. The results were divided into two groups, the first group corresponds to a density of $(1\text{-}1.2) \times 10^{19}\ m^{-3}$ (solid circles), and the second group between $(1.25\text{-}1.45) \times 10^{19}\ m^{-3}$ (open circles). What is clear is the behavior of the electron temperature to the density, in this region of plasma, shown by line fit, the electron temperature decreases as we increase the density. From this we can deduce that the results obtained by the ECE diagnostic are in full agreement with what was expected in the plasma of TCABR. After careful reviews of the electron temperature, measured simultaneously by the ECE and ITS diagnostics of a relatively large number of discharges, discrepancies were found in many of them. The question is: what is happening so that there is an apparent contradiction in the temperature measurement made by both diagnostics? To provide an answer to this question, more detailed reviews are carried out. Then we use the experimental results obtained for ohmic discharges, such as the ECE

radiometer, ITS, and Mirnov coils to thereby obtain information on electron temperature in the center of the plasma column. For comparison only are selected plasma discharges doing not overstep the limits of cutting the ECE diagnostic, imposed by the electron density, i.e. line-averaged electron density range $\bar{n}_e=(1-1.5)\times10^{19}\ m^{-3}$. For line density, $\bar{n}_e>1.5\times10\ m^{-3}$ (the central density $n_{e0}>2.5\times10^{19}\ m^{-3}$) the cutoff in ECE radiation was observed. In Figure 5, showing two typical discharges; the first with no MHD activity (shot 24472) and the second with strong MHD activity (shot 24231). The dashed line indicates the instant it is connected to the Thomson scattering diagnostic (*t=73 ms* for 24472 and *t=90ms* for 24231 discharge); this instant of time coincides with the measurement of electron temperature for both diagnostics. The evolution of temporal profiles in shot 24231, we can see clearly that the MHD oscillation, Mirnov coil signal, results in a decreased electron temperature, the radiometer ECE signal.

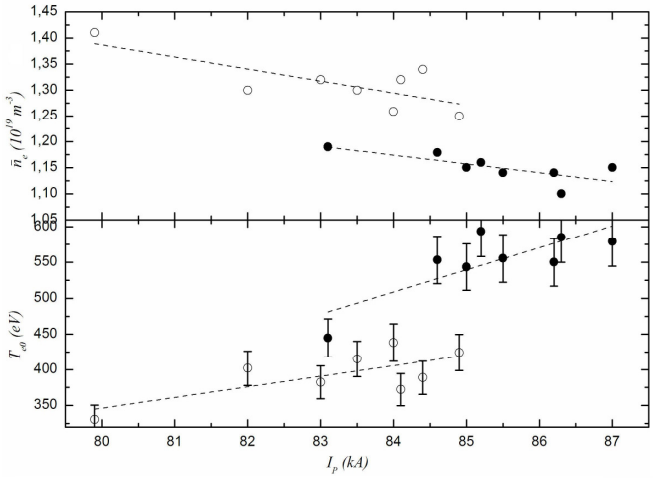

Figure 4. Overall result of the electron density and temperature in the center of the plasma column for ohmic discharges in TCABR tokamak. Top: the line-averaged density versus current plasma. Bottom: the central electron temperature, measured with ECE diagnostic, versus the current plasma. The lines indicate fits through the data.

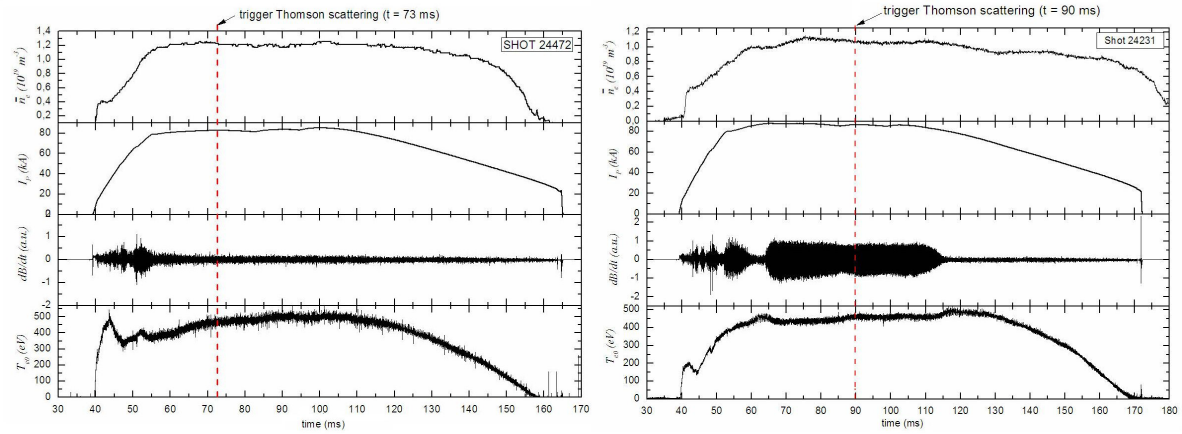

Figure 5. Typical discharge in TCABR tokamak, shot 24472 with very low MHD activity and the shot 24231 with strong MHD activity. Shows the temporal profiles obtained for of averaged-line density ($\bar{n}_e$), current plasma *(I_P),* Mirnov coil and electron temperature (signal ECE). The dashed line indicate trigger Infrared Thomson scattering system.

Making up the Fourier analysis of time signals of ECE in both discharges (Fig. 6a), we observe the presence of dominant frequency of *~2.4 kHz* (and subsequent harmonics), which corresponds to the oscillation frequency of the sawtooth (safety factor *q<1*). The sawtooth oscillations appear in shot 24472, during ohmic discharge phase (~60ms to ~140ms), and shot 24472 appear early (*t~60 ms*), corresponding to initial phase of the discharge with duration approximately of *10ms*, and final phase (*t~110 ms*) (Fig. 6b). Then performed the Fourier spectral analysis of signals measured by Mirnov coils in both discharges (Fig. 6c), proved the existence of a dominant mode with a frequencies of 12.5

kHz to 14 kHz. This frequency is not present in the spectrogram ECE for shot 24472. The same is not true for shot 24231, where the ECE signals and Mirnov coils present similar frequency ~12.5 kHz, in spectral graphs, constant during the time intervals (*~70 ms* to *~110 ms*). The position feedback system of TCABR guarantees that substantial horizontal and vertical displacements of the plasma column do not occur in this time interval.

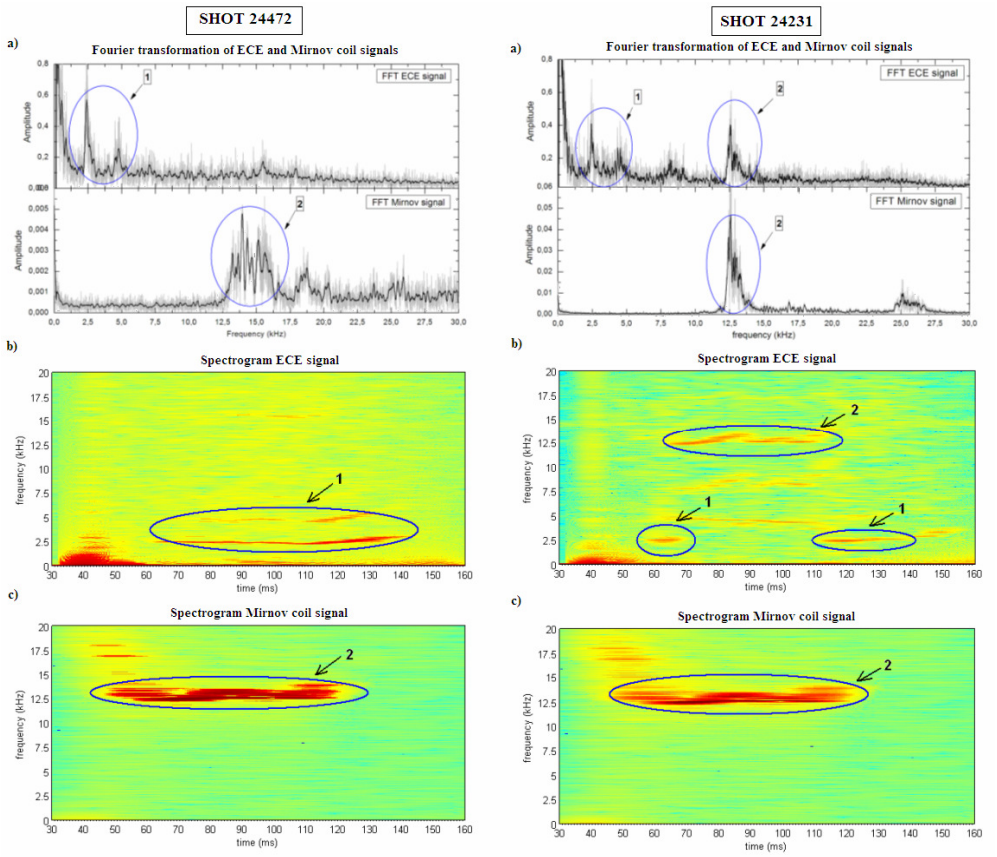

Figure 6. a) Fourier transformations of ECE and Mirnov coil signals, b) power spectrum of ECE radiometer data located central plasma column and c) power spectrum of Mirnov coil located on the outboard midplane, for shots 24472 and 24231 respectively.

The Figures 7 shows the central electron temperature, measured simultaneously by Thomson scattering and ECE diagnostic, in the ohmic phase as a function of density, In Figure 7a, the Thomson scattering data confirm the measured values by ECE when there is no MHD activity. The opposite occurs when there is a strong MHD activity; this is evident in Figure 7b.

5. Discussions and Conclusion

The electron temperature is measured by Infrared Thomson scattering and ECE diagnostics in TCABR experiments. Analyzing the temperature of a set discharges, we can confirm that the temperature obtained by ECE diagnostics decreases with increasing of the electron density due to imposing a cutoff layer. Some discrepancies appear in temperature measurements with the ECE and ITS diagnostics when they are carried out simultaneously. From a detailed analysis of the results, we conclude that the signals in discordant measurements have a strong MHD activity, which appears in the temperature profile, this result is observed in the analyzed frequency ECE spectrum.

An important factor is that ECE and ITS diagnostics are positioned along toroidal direction with a angle gap *≈120* degrees, that does not give possibility to observe the same plasma region. Others important differences in this analysis are; the temporal resolution of the diagnostics (ECE *≈10μs* and

ITS *≈50ns*) and observed plasma volume by ECE *≈6.46cm*^{3} and by ITS *≈0.13cm*^{3}. The parameters of one can conclude that the measured temperature by the ITS is a instantaneous measurement, and the electron temperature measured by ECE has temporal and spatial averaging.
In summary, we conclude that both diagnostics appear as different during MHD activity. The ITS be measured at a point of radius (with higher spatial resolution), and in a very short time interval likes a few nanoseconds, and ECE observe the emission of radiation from a larger region of the plasma and during the time interval approximately 200 time greater. In the sense, this discrepancy in the measurement of electron temperature during MHD activity happens in reality because the temperature is acquired by both diagnostics in the different manner, and is inherently influenced by parameters of a technical nature.

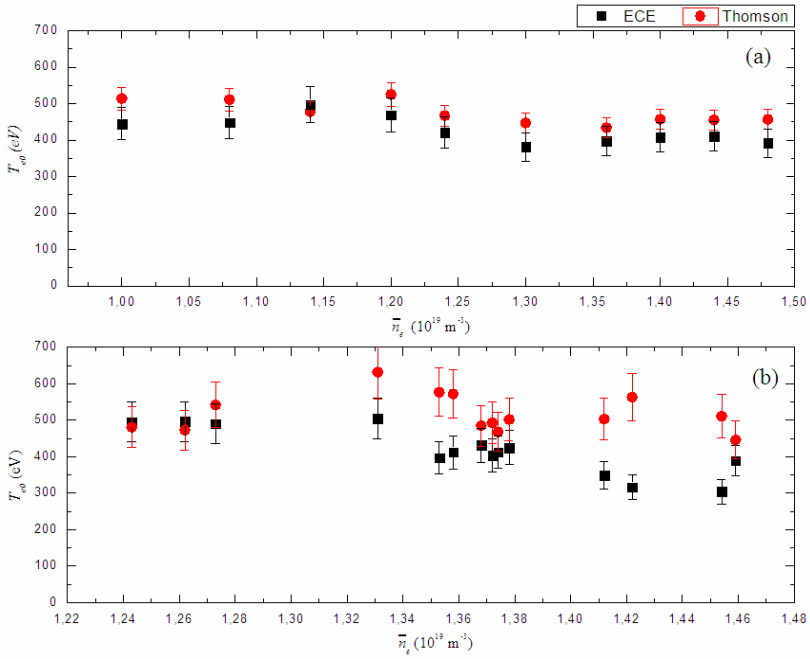

Figure 7. (a) Electron temperature without MHD activity e (b) temperature perturbed by large MHD mode activity. ECE radiometer temperature (solid squares), Infrared Thomson scattering temperature (solid circles). The errors bars for T_e in both diagnostic are of the order of 10%.

Acknowledgments
This work was partially supported by CNPq (National Council for Research and Development – Brazil) and by FAPESP (Foundation for Supporting Research of the State of São Paulo). The authors wish to thank to the "Instituto Superior Técnico – IST" (Portugal) for collaboration in the implementation of the Thomson scattering diagnostic and tokamak TCABR team.

References
[1] Galvão R M O, Kuznetsov Yu K, Nascimento I C, et al. 2001 *Plasma Physics and Controlled Fusion*. v. **43**, pp. 1181
[2] Ruchko L F, Lerche E A, Galvão R M O, et al. 2002 *Brazilian Journal of Physics*. V. **32** pp 57
[3] Severo J H F, Nascimento I C, Tsypin V S, et al. 2004 *Physics of Plasma* **11**(2) 846
[4] Heller M V A P, Caldas I L, Ferreira A A, et al. 2005 *Czechoslovak Journal of Physics* **55** 265
[5] Nascimento I C, Kuznetov Yu K, Guimarães-Filho Z O, et al. 2007 *Nuclear Fusion* **47**, 1570
[6] Severo J H F, Tsypin V S, Galvão R M O, et al. 2002 *Brazilian Journal of Physics* v.**32**, pp. 13
[7] Severo J H F, Nascimento I C, Kuznetov Yu K, et al. 2007 *Review of Scientific Instruments* **78** 043509
[8] Severo J H F, Nascimento I C, Kuznetov Yu K, et al. 2009 *Nuclear Fusion* **49**, 115026
[9] Alonso M P, Figueiredo A C A, et al. 2010 *Journal of Physics: Conference Series* **227** 012027
[10] da Silva R P, Fonseca A M M, Vuolo J H, et al. 2004 *Brazilian Journal of Physics* v. **34**, 1771
[11] Alonso M P, Bemi L A, Severo J H F, et. al., 2008 *Plasma and Fusion Science* **996**, 192